pH-sensitive hydrazone linked doxorubicin-nanogels via polymeric activated ester scaffolds: synthesis, assembly, in vitro and in vivo evaluation in tumor bearing zebrafish

Alexandra Van Driessche[1$], Agnese Kocere[2$],Hannelien Everaert[1], Lutz Nuhn[1,3], Simon Van Herck[1], Gareth Griffiths[2*], Federico Fenaroli[2*], Bruno G. De Geest[1*]

1 Department of Pharmaceutics, Ghent University, 9000 Ghent, Belgium and Cancer Research Institute Ghent (CRIG)

2 Department of Biosciences, University of Oslo, 0371 Oslo, Norway

3 Max-Planck-Institute for Polymer Research, Mainz, Germany

$ these authors contributed equally to this work

* g.w.griffiths@ibv.uio.no, federico.fenaroli@ibv.uio.no, br.degeest@ugent.be

Abstract

Nanoparticle conjugation is a powerful method to reduce the side effects of anticancer agents such as doxorubicin by altering the pharmacokinetic profile of the drug. Nanoparticles can prolong circulation time and could also promote enhanced accumulation in tumors, either passively via the EPR effect or actively when decorated with targeting motifs. For the particular case of doxorubicin, hydrazone-based conjugation chemistry is popular, but commonly involves laborious chemical transformation steps[1]. Here we report on a straightforward route for the synthesis of hydrazine-based doxorubicin-polymer conjugates starting from a polymeric activated ester scaffold onto which doxorubicin-reactive hydrazide moieties are introduced by simple treatment with hydrazine. Using block copolymers composed of hydrophobic reactive ester block we demonstrate a simple route to assemble core-crosslinked doxorubicin-loaded nanoparticles. The latter largely retain their bioactivity *in vitro*. In a zebrafish embryo ´pre-murine´ *in vivo* model we demonstrate a dramatic reduction in systemic toxicity of doxorubicin upon nanoparticle-conjugation and also demonstrate enhanced tumor accumulation and tumor growth reduction.

INTRODUCTION

Doxorubicin is amongst the most widely used anticancer agents[2,3]. Like other anthracyclines, it mainly acts through intercalation with the cancer cell DNA, leading to disruption of transcription and replication processes, resulting in cell death[4,5]. However, like most chemotherapeutics, doxorubicin suffers from reduced therapeutic efficiency due to occurrence of harmful side effects[6]. These include nausea, hair loss, bone marrow suppression, drug resistance and most notably, cardiotoxicity[7,8]. Stemming from a lack of selectivity toward cancer cells, these limitations could be overcome by the development of more advanced doxorubicin formulations[9]. This can be accomplished through formulation of the drug in nanoparticles. Nanoparticle formulations could provide a more controlled release of the drug load, and hence reduce peak levels or, could in ideal cases also promote increase drug deposition in tumor tissue by virtue of the enhanced permeability and retention (EPR) effect[6,10–12]. However, the relevance of the EPR effect for passive targeting of a broad range of tumors in human patients is currently under debate[13]. Currently two nanoparticulate liposomal doxorubicin formulations have been commercialized: Doxil/Caelyx (PEGylated) and Myocet (non-PEGylated)[14,15]. These formulations are based on physical drug entrapment, which entails the risk of systemic release upon intravenous administration[16]. This risk can be mitigated through chemical conjugation to nanocarriers such as responsive polymeric nanoparticles, which gives access to a more selective drug release[17–19].

In contrast to physical formulation of a drug through hydrophobic interaction (e.g. in the core of amphiphiles) or inclusion (e.g. in the hollow void of liposomes), chemical conjugation is a much more robust strategy as it avoids disassembly of the carrier itself or the carrier-drug complex in response to dilution and interaction with serum proteins upon entry into blood circulation[16,20]. In this regard, antibody-drug conjugates are a successful example of how potent cytotoxic drugs can be more selectively delivered to tumor cells that overexpress a specific surface marker[21]. Besides that, many other systems based on polymeric/nanoparticles drug conjugates without a small or macromolecular targeting ligand are currently under (pre)clinical development[10,22]. A key feature in successful macromolecular design of polymer-drug conjugates is to insert a degradable linker between the drug molecule and the polymer backbone, which allows for gradual drug release (typically using hydrolysis of ester linkages) or to release the drug in response to specific stimuli in tumor tissue, or in endosomes upon cellular uptake[9]. For the latter purpose, cathepsin-cleavable peptides, acid-cleavable linkers such as hydrazones, ketals, substituted esters and reduction/disulfide exchange-sensitive disulfides and self-immolative linkers derived thereof have been explored[23–34]. Akin to many of these strategies are challenging procedures required to synthesize complex macromolecular

structures composed of drug, linker and polymer, and subsequent assembly into 3D structures.

In this study, we present a straightforward approach based on polymeric activated ester scaffolds for the synthesis of polymer- and nanoparticle-doxorubicin conjugates using acid sensitive hydrazone linkages[35]. In contrast to previous reports using acetoxime acrylate[36] as precursor for the synthesis of polymeric hydrazones, the use of pentafluorophenyl (PFP) base activated ester scaffolds allows to perform nanoparticle assembly of block copolymers based on solvophobic interaction of the poly(pentafluorophenyl acrylate) blocks, hence highlighting the versatile nature of PFP-ester chemistry for the design of complex macromolecular architectures.

Hydrazones exhibit strongly accelerated hydrolysis at mildly acidic pH and are therefore well suited for both endosomal and intra-tumoral drug release[3,37]. A requisite for the formation of a hydrazone bond is the presence of a carbonyl or hydrazide in the drug molecule and the corresponding counterpart (i.e. hydrazide or carbonyl) on the polymer backbone. A well-known example of a hydrazone-based polymer drug conjugate is doxorubicin-poly(N-hydroxypropylmethacrylamide) which has reached phase I/II clinical testing[38]. Doxorubicin-polymer conjugates are mostly obtained through copolymerization followed by several post-modification reactions. The resulting structures contain both hydrophilic repeating units to confer water-solubility and hydrazide moieties for drug conjugation. For more advanced structures, additional reactive moieties can be included as needed e.g. crosslinking or labeling with tracer molecules[39].

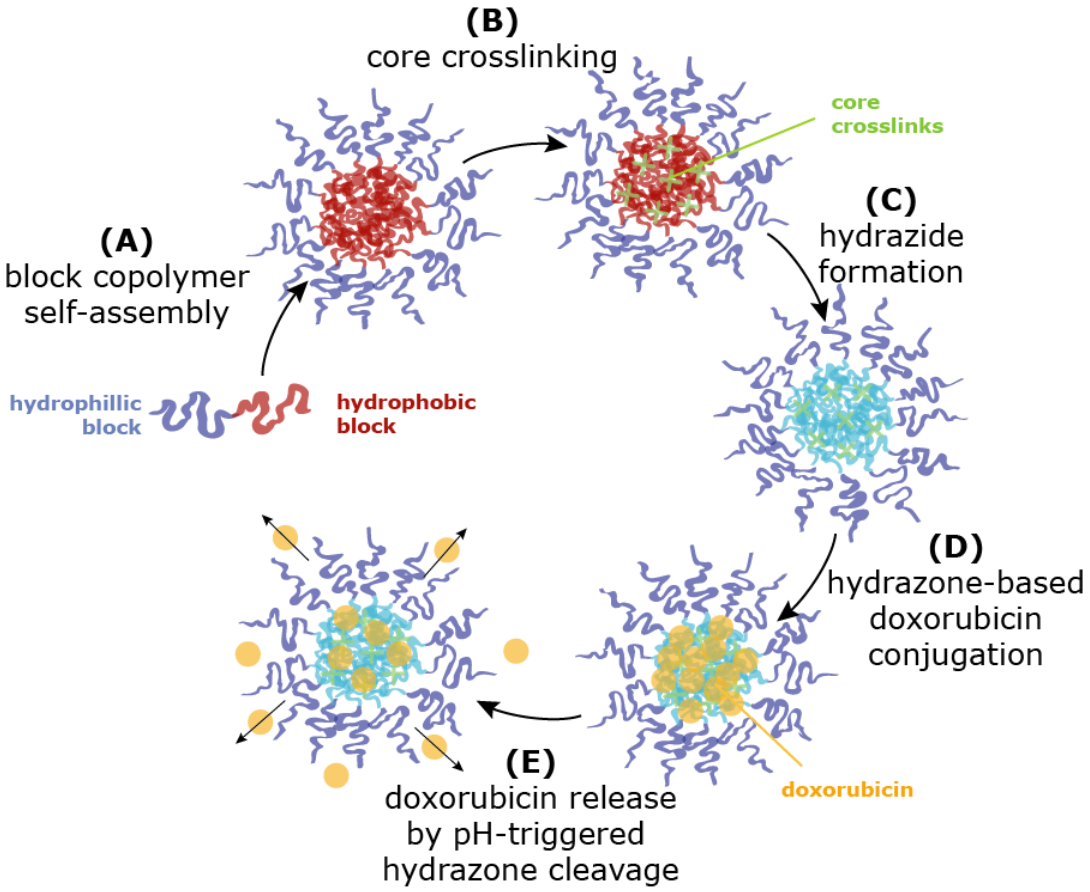

Figure 1. Schematic representation of **Nanogel^{DOX}**. **(A)** Block copolymers composed of poly(pentafluorophenylacrylate) as hydrophobic block are self-assembled by solvophobic interaction into micellar nanoparticles in DMSO. The later solvent allows for subsequent core-modification of the nanoparticles without competing hydrolysis of the activated ester moieties, opposed to when self-assembly would be performed in aqueous medium. **(B)** For core-modification, cross-linking is induced by bisamines that form inter- and intra-chain amide bonds. **(C)** Remaining pentafluorophenyl esters are transformed into hdyrazides and hydrophilic inert repeating units by reaction with hydrazine and aminoethanol. **(D)** After purification to remove unreacted species and by-products, doxorubicin is conjugated via its carbonyl moiety to the hydrazide moieties in the nanogel core by hydrazone-bond formation. **(E)** Doxorubicin is released from the nanogels by pH-triggered hydrolysis of the hydrazone bond between the polymer backbone and doxorubicin.

Our approach, depicted in **Figure 1**, is based on amphiphilic block copolymers consisting of a hydrophobic activated ester poly(pentafluorophenyl acrylate)[40] block and a hydrophilic poly(N,N-dimethylacrylamide) block. These block copolymers self-assemble into nanoparticles in protic apolar solvents that can be cross-linked with bisamines[41–44]. We demonstrate that the activated esters can very efficiently be converted into hydrazides by treatment with hydrazine. After crosslinking, the latter allow for chemical conjugation of doxorubicin via an acid-labile hydrazone bound, yielding stable doxorubicin-loaded

nanogels. We demonstrate cellular uptake of doxorubicin-loaded nanoparticles *in vitro* and with a minor decrease in cytotoxic activity relative to soluble doxorubicin. *In vivo* experiments in zebrafish embryos, a transparent vertebrate system that allows for straightforward high resolution whole animal fluorescence imaging of nanoparticle fate[45,46], demonstrate a dramatic reduction in systemic toxicity relative to the free drug. In zebrafish model[45] xenografted with tumor cells, we show that the reduced drug toxicity upon nanoparticle encapsulation is accompanied by the selective accumulation of the nanoparticles in tumor tissue and a decrease in tumor growth.

EXPERIMENTAL

Materials

All chemicals were purchased from Sigma-Aldrich, unless stated otherwise. Pentafluorophenyl acrylate (PFP) and 2-(butylthiocarbonothioylthio)propanoic acid (PABTC) were synthesised as previously reported[44,47]. Deuterated solvents for NMR measurements were purchased from Deutero GMBH. Spectra/Por 6 dialysis tubing with a MWCO of 3.5 kDa were ordered from Spectrum Labs. Doxorubicin was obtained from Lancrix. Cyanine5 amine was purchased from Lumiprobe. Dulbecco's phosphate buffered saline (PBS), Dulbecco's modified Eagle Medium (DMEM), Fetal bovine serum (FBS), L-glutamine, penicillin, streptomycin, Hoechst and Alexa Fluor 647 phalloidin were purchased from Invitrogen. SKOV-3 and B16 cells were supplied by ATCC.

Instrumentation

^{1}H- and ^{19}F-NMR spectra were recorded on a Bruker FT NMR spectrometer at 300 or 500 MHz.

Dynamic light scattering (DLS) measurements were performed on Zetasizer Nano S (Malvern Instruments Ltd) equipped with a HeNe laser (λ=633 nm) and detection at a scattering angle of 173°. UV/Vis measurements were performed on a UV-1650PC (Shimadzu) and an Epoch 2 microplate reader (BioTek).

Fluorospectrometry measurements were carried out on an EnVision Multilabel plate reader from Perkin Elmer.

GPC was used for the determination of molecular weights and molecular weight distributions of polymers derived from RAFT polymerization performed on a Waters Instrument with an RI detector (2414 Waters), equipped with a Polymer Standards Services GPC precolumn (PSS SDV analytical 5 µ 8,0 x 50 mm) and three Polymer Standards Services GPC serial columns (PSS SDV analytical 1000 Å, 5 µ 8,0 x 300 mm, PSS SDV analytical 100000 Å, 5 µ 8,0 x 300 mm, PSS SDV analytical 1000000 Å, 5 µ 8,0 x 300 mm) at 35 °C. Polystyrene

standards were used for calibration. Chloroform stabilized with ethanol was used as eluent at a flow rate of 1 mL·min^{-1}. Samples were injected using a Waters 717plus auto sampler.

Synthesis of pDMA

A dry Schlenk tube was filled with DMA (496 mg, 5.0 mmol), PABTC (24 mg, 0.1 mmol) and AIBN (1.6 mg, 0.010 mmol). Anhydrous dioxane was added to reach a total volume of 5 mL, dissolving all components. This solution was subjected to 5 freeze-pump-thaw cycles before initiating polymerization at 80°C for 3 hours under vacuum and continuous stirring. Monomer conversion was determined using ^{1}H-NMR. The polymer was purified by triple precipitation in a 1:1 hexane:diethyl ether mixture. The obtained yellow powder was dried under high vacuum (495 mg, 0.099 mmol).

Synthesis of pDMA-b-pPFPA

A dry Schlenk tube was filled with PFPA (714 mg, 3.0 mmol), pDMA (333 mg, 0.067 mmol) and AIBN (2.2 mg, 0.013 mmol). Anhydrous dioxane was added to reach a total volume of 3 mL, dissolving all components. This solution was subjected to 5 freeze-pump-thaw cycles before initiating polymerization at 80°C for 3 hours under vacuum and continuous stirring. Monomer conversion was determined using ^{19}F-NMR. The polymer was purified by triple precipitation in ice-cold hexane. The obtained slightly yellow powder was dried under high vacuum (877 mg, 0.067 mmol).

Nanogel assembly

Crosslinking

800 mg pDMA-b-pPFPA (2.1 mmol reactive esters, 1.0 eq.) was divided equally over 2 dry round bottom flasks, equipped with a stir bar followed by the addition of 40 mL anhydrous DMSO under a nitrogen atmosphere. Ultrasonication (3 hours at room temperature) was applied to dissolve the polymer and allow micelle formation by solvophobic interaction between the pPFPA polymer blocks. In case of fluorescent labelling, 0.0050 eq. cyanine5-amine (5.1 µmol, 3.4 mg) and 0.030 eq. TEA (31 µmol) were added to 1 of the flasks and the solution was incubated at 40°C for 3 days **(Nanogel^{Cy5})**. After 3 days, 0.25 eq. (ethylenedioxy)bis(ethylamine) (0.26 mmol) and 5.0 eq. TEA (5.2 mmol) were added to each dispersion and the mixtures were stirred for 16 hours at 50°C to achieve crosslinking.

Incorporation of hydrazides

After crosslinking, an excess of 2.5 eq. ethanolamine (2.6 mmol) and 2.5 eq. hydrazine (2.6 mmol) was added to the crosslinked nanoparticle solution to ensure complete removal of all reactive PFP groups in presence of 15 eq. TEA (16 mmol).

The reaction mixture was incubated at 50°C for another 20 hours before purification by dialysis. Dialysis was conducted using a dialysis membrane with a molecular weight cut-

off of 3.5 kDa in a 1:1 methanol:water mixture for three days, while gradually shifting the dialysis medium towards pure water. After dialysis, the nanogels were freeze-dried and redispersed in PBS to be analyzed by DLS.

Doxorubicin conjugation (Nanogel^{DOX}).

Nanogels and 0.5 eq. doxorubicin for each hydrazide group were dissolved in anhydrous methanol at a doxorubicin concentration of 3.3 mM. Acetic acid (11 eq.) was added to aid the conjugation reaction[48]. This mixture was reacted overnight in the dark at room temperature, before being transferred to a dialysis membrane and dialyzed against 1L of a 0.05% ammonia buffer (pH 9.1). After 3 days of dialysis, the mixture was lyophilized.

Doxorubicin content determination

The amount of doxorubicin conjugated to the polymers was determined by UV-vis spectrometry at a wavelength of 481 nm. A standard concentration curve with doxorubicin concentrations between 0.005 and 0.1 mg/mL was prepared in PBS. Samples of each doxorubicin containing nanoparticle were prepared in PBS and analyzed at 481 nm. The doxorubicin content of the different formulations was determined by comparing it to the values of the standard curve.

Doxorubicin release

A nanoparticle formulation containing 0.5 mg/mL **Nanogel^{DOX}** was prepared in PBS. The formulation (1.5 mL) was transferred into a dialysis membrane and dialyzed against 40 mL PBS or 50 mM acetate buffer pH 5. The dialysis tubes were incubated at 37°C and samples were collected by withdrawing 2 mL of the dialysis medium and replacing it with 2 mL of fresh medium. Samples were taken at 1, 2, 4, 6, 24, 48, 72, 96, 120 and 168 hours. The experiment was done in triplicate. The doxorubicin content of each sample was determined by fluorescence spectrometry at an excitation wavelength of 480 nm and an emission wavelength of 590 nm. Calibration curves in both buffers are shown in **Figure S9** in Supporting Information.

In vitro cell experiments

Cell culture

SKOV-3 human ovarian cancer cells and B16 murine melanoma cells were cultured in DMEM supplemented with 10% FBS, 2 mM L-glutamine, 50 µg/mL streptomycin and 50 units/mL penicillin. Cells were incubated in a controlled, sterile environment at 37°C, 95% relative humidity and 5% CO_2.

Cytotoxicity

In vitro cytotoxicity was determined by MTT assay. SKOV-3 and B16 cells were seeded in 96-well plates (10 000 cells per well, suspended in 200 µL cell medium) and incubated

overnight. The next day, 50 µL formulation, DMSO (positive control = 0% viability) or PBS (negative control = 100% viability) was added to the wells, followed by a 72h incubation period. Formulations of soluble doxorubicin and **Nanogel^{DOX}** in PBS were prepared with doxorubicin concentrations between 500 µg/mL and 2.5 ng/mL. After 72 hours, the medium was aspirated and the cells were washed with 200 µL PBS. After aspiration, 100 µL MTT working solution was added to each well and the cells were incubated for 2.5 hours. The MTT working solution was prepared by dissolving 100 mg thiazolyl blue tetrazolium bromide in 20 mL PBS, followed by membrane filtration (0.22 µm) and 5-fold dilution in cell culture medium. After 2.5 hours, the MTT working solution was aspirated and the formed formazan crystals were dissolved in 50 µL DMSO. The absorbance of each well was measured at 590 nm. The absorbance of the blank wells was used as a positive control and thus subtracted from all values.

Cellular uptake and intracellular fate

SKOV-3 cells were seeded in confocal dishes (5 000 cells per dish, suspended in 200 µL cell medium) and incubated overnight. The next day, 300 µL sample was added to each well. Samples of soluble doxorubicin and **Nanogel^{DOX}** in PBS were prepared with doxorubicin concentrations of 5 µg/mL. The dishes were incubated for 48h before fixation, using 4% PFA. All samples were washed with PBS and stained with Hoechst and Alexa Fluor phalloidin 488. This staining solution was prepared by adding 20 µL of 1 mg/mL Hoechst stock solution and 50 µL of a 200 units/mL Alexa Fluor phalloidin 488 stock solution to 2 mL PBS. Following another washing step, the cells were imaged using a Leica DMI6000B microscope with a 63X, 1.40 NA objective, attached to an Andor DSD2 confocal scanner.

In vivo experiments in zebrafish embryos

Systemic toxicity testing

Samples of free doxorubicin and **Nanogel^{DOX}** were diluted in a deionized water solution containing a 2% polyvinylpyrrolidone (PVP) in order to reach a doxorubicin concentrations of 2 mg/mL or 4 mg/mL. For each condition 20-30 zebrafish embryos were injected with sample volumes between 0.5 and 20 nL, 3 days after fertilization. The diluting medium alone was used as control. Over the next 6 days, the fish were incubated at 32°C and assessed for their survival in each treatment condition.

Tumor accumulation

B16 mouse melanoma cells expressing RFP or GFP were injected in zebrafish embryos zebrafish embryos at 2 days post fertilization and incubated at 32°C. Five days after the xenotransplant we intravenously injected 5 nL of a 4 mg/mL solution of **Nanogel^{Cy5}**. The tumor region in the zebrafish was then imaged at 1 day post injection using the confocal

microscope Zeiss LSM 880 with Fast AiryScan using a Leica LD LCI 25X/0.8 objective with oil immersion.

Therapeutic evaluation

At two days post fertilization, B16 mouse melanoma cells expressing RFP were injected into the neural tube of zebrafish embryos and subsequently incubated at 32°C. 3 days post fertilization, the fish were injected with free doxorubicin 4 mg/kg or nanogel-conjugated doxorubicin at 40 mg/kg. As control groups we injected zebrafish larvae with an equivalent concentration of doxorubicin-free nanogels or with the diluting medium alone. Five days post injection, the tumors were imaged using a Leica DFC365FX stereo microscope with a 1.0x plan apo lens. In order to assess the effect of the treatment on tumor growth, the florescence of the cancer cells in each group were compared using the software Image J. Zebrafish larvae dying because of toxicity were removed and not included in the final graph.

RESULTS AND DISCUSSION

Amphiphilic block copolymers composed of N,N-dimethylacrylamide (DMA) and pentafluorophenylacrylate (PFPA) were synthesized by RAFT polymerization using 2-(butylthiocarbonothioylthio)propionic acid (PABTC) as chain transfer agent (CTA) and AIBN as radical initiator (**Scheme 1**). The hydrophilic pDMA block was first synthesized with a targeted degree of polymerization (DP) of 50. The conversion of DMA was determined by ^{1}H-NMR to be 96%, yielding p(DMA$_{48}$), which subsequently served as macroCTA for the next block. For the latter, PFPA was RAFT polymerized targeting a DP of 45. ^{19}F-NMR revealed a monomer conversion of 74%, resulting in a p(DMA$_{48}$-*b*-PFPA$_{34}$) polymer. The size distribution of the (block) copolymers were analyzed by size exclusion chromatography (SEC) and the polymer properties are shown in **Table 1.**

Scheme 1. Synthesis of poly(DMA$_n$) macroCTA and p(DMA)-*b*-p(PFPA) via RAFT polymerization.

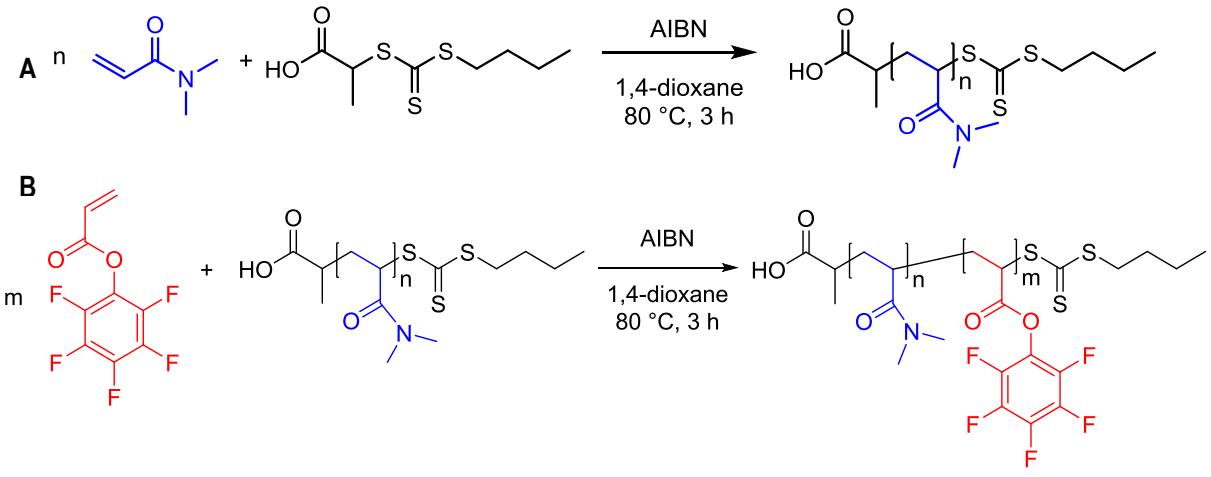

Scheme 2. Crosslinking (green) of p(DMA)-*b*-p(PFPA) (A) and substitution of remaining active esters with hydrazine and ethanolamine (red) (B).

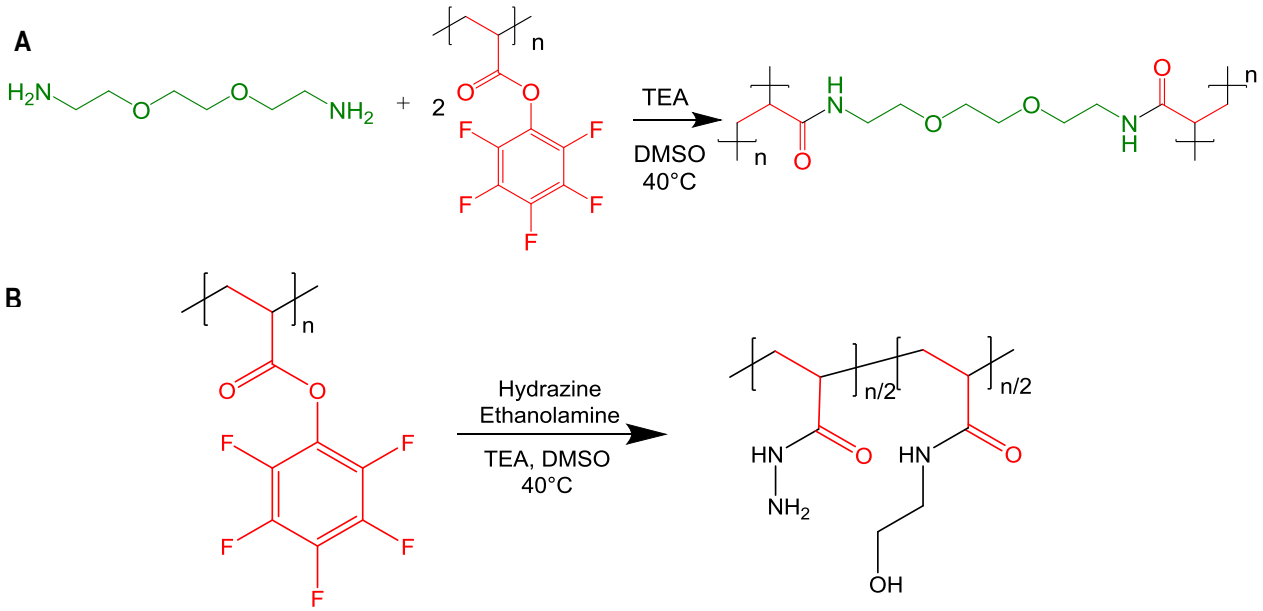

Scheme 3. Conjugation of doxorubicin (orange) to hydrazide groups, forming a hydrazone bond.

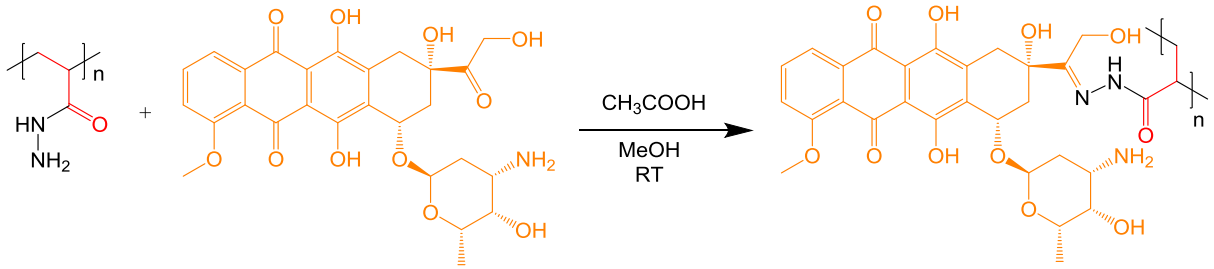

Table 1. Compositional data of the synthesized polymers.

	[monomer]/[CTA]	Conversion (%) [a]	DP (NMR)	MW (kDa) [A]	MW (kDa) [B]	Đ [B]
p(DMA)	50	96	48	5.0	3.9	1.13
p(DMA)-b-poly(PFPA)	45	74	34	13	6.3	1.51

[A]Calculated using ^{1}H NMR. [B]Analyzed by SEC

Table 2. Z-average diameter and PDI during the synthesis of the nanogels as measured by DLS.

	Solvent	Z-average (±SD)	PDI (±SD)	ζ-potential (mV)
before crosslinking	DMSO	91 (±9)	0.620 (±0.177)	/
after crosslinking	DMSO	74 (±1)	0.458 (±0.021)	/
after freeze drying	PBS	85 (±6)	0.605 (±0.111)	-7.35 (±6.63)
after doxorubicin conjugation	PBS	75 (±0.4)	0.338 (±0.007)	-8.37 (±8.08)

The block copolymer was dissolved in DMSO and dynamic light scattering (DLS) revealed the formation of nanoparticles with a mean hydrodynamic diameter of 91 nm. Although hydrolysis of the PFP esters cannot be fully excluded, this is minimal when using anhydrous solvents. Moreover, PFP-esters are known to be resilient towards hydrolysis while showing high reactivity towards primary amines[40]. The nanoparticles were then subjected to a core-crosslinking step by the addition of 2.2′-(ethylenedioxy)bis(ethylamine) (**Scheme 2**), resulting in the formation of amide bonds between the PFPA repeating units. In this reaction, 0.25 equivalents of 2.2′-(ethylenedioxy)bis(ethylamine) relative to the number of reactive esters were added. Crosslinking is intended to ´lock´[49] the nanoparticle state, followed by reacting the remaining PFP-esters with a 5 eq. excess of a 50:50 equimolar mixture of hydrazine and 2-ethanolamine. A small hydrophilic amine such as 2-ethanolamine should render the core of the nanoparticles sufficiently hydrophilic and, hence, promote full hydration upon transfer to aqueous medium by dialysis at the final step of the formulation process. Whereas, modification with a small hydrophobic amine would yield amphiphilic structures that will self-assemble into micellar nanoparticles in aqueous medium, it is important to note that non-crosslinked block copolymer micelles are commonly prone to disassembly upon dilution in complex physiological media[49]. Moreover, doxorubicin is insufficiently hydrophobic to drive assembly into micelles with high physiological stability. In the present study, for a proof-of-concept, we focused only on a non-degradable crosslinker. However, the synthesis of degradable nanogels can be achieved using bisamine crosslinkers containing a degradable bond such as a disulfide or a ketal[42,43,50,51]. For the synthesis of fluorescently labelled nanogels (**Nanogel^{Cy5}**), 2% of the reactive esters on the polymer were substituted with cyanine5-amine prior to crosslinking. We chose cyanine5 as a labelling agent because its fluorescence excitation and emission spectra do not, contrary to rhodamine and fluorescein, show overlap with the spectra of doxorubicin[52].

To address potential concerns regarding additional crosslinking upon reaction of the PFP-esters with hydrazine and 2-aminoethanol[53], a control experiment was performed in which bisamine-crosslinking was omitted and only the 5 eq. excess of hydrazine and 2-ethanolamine (50:50) was added. After purification, the reaction product was measured by DLS, revealing a size distribution corresponding to unimers (**Figure S8** in Supporting Information). Hence we concluded that neither hydrazine nor 2-aminoethanol induced additional crosslinking, which is in line with our previous findings[42] on substitution of polymeric activated ester scaffolds with 2-aminoethanol.

After dialysis to remove unreacted species and released pentafluorophenol, the hydrazide groups in the nanogel core were used for doxorubicin conjugation through the formation

of an acid-labile hydrazine bond (**Scheme 3; Nanogel^{DOX}**). This linkage provides stable conjugation at neutral, physiological pH conditions, but shows accelerated hydrolysis at mildly acidic pH, as encountered in the tumor microenvironment and in endolysosomal vesicles (e.g. early endosomes have a pH around 6.2; lysosomes around 5 or below[54]). Towards this goal, we prepared doxorubicin-conjugated nanogels with doxorubicin equivalents corresponding to half of the hydrazide groups on the nanogels added for conjugation. After dialysis against water, the final concentration of doxorubicin conjugated to the nanogels was determined by UV/Vis spectrometry to be 19 % (w/w). Determination of the doxorubicin content was done by UV/Vis spectrometry, and not fluorimetry, to avoid interference with fluorescence quenching of the doxorubicin inside the nanogel core.

To assess the suitability of the hydrazone bond between the polymer backbone and the doxorubicin for accelerated drug release at slightly acidic conditions, we loaded the **Nanogel^{DOX}** in dialysis tubes and placed these in either neutral or slightly acidic medium at 37°C. The amount of doxorubicin released in the medium outside the dialysis bags at either pH was quantified by fluorimetry over the next 6 days. Detection via fluorimetry was prefered over UV/Vis spectrometry due to its lower limit of detection, necessary to quantify the low concentrations in this experiment. Calibration curves at both pH values are shown in **Figure S9** in Supporting Information. **Figure 2** shows that doxorubicin release occurred at pH 5, whereas at the physiological pH of 7.4, doxorubicin release was significantly less, even after 6 days. These results demonstrate the stability of the hydrazone bound at neutral physiological conditions, while confirming its suitability for drug release at acidic conditions. When injected into the blood circulation, doxorubicin is expected to remain predominantly conjugated to the nanogels and become released much faster upon entering the tumor environment or upon endosomal uptake by cancer cells due to accelerated hydrazone cleavage under acidic conditions[54].

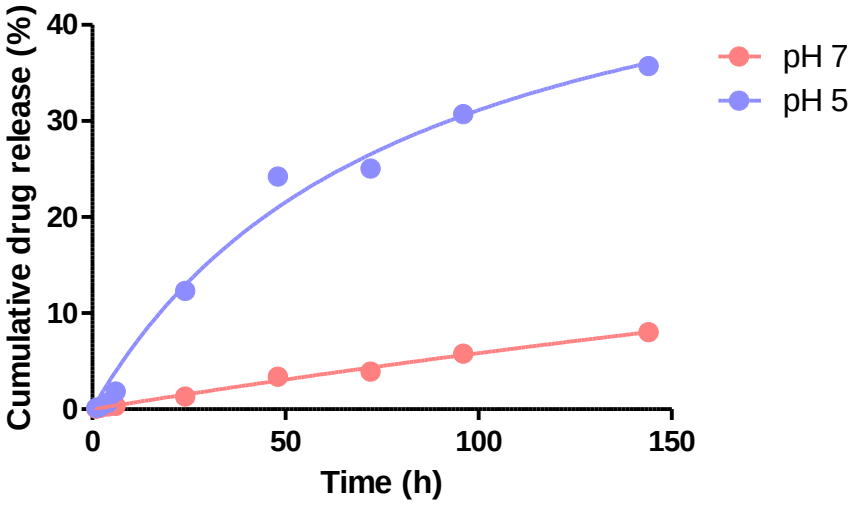

Figure 2. Cumulative release profile doxorubicin from **Nanogel^{DOX}** formulation at physiological (red) and endo-lysosomal acidic (blue) pH.

Cellular uptake of **Nanogel^{DOX}** was first assessed in vitro on SKOV-3 human ovarian cancer cells via confocal microscopy, taking advantage of the intrinsic fluorescence of doxorubicin (**Figure 3**). Whereas doxorubicin in soluble form exhibited accumulation predominantly in the cell nucleus, **Nanogel^{DOX}** showed a much more punctuated pattern, with only part of the fluorescence signal being localized to the nucleus. Free doxorubicin can permeate across cell membranes and hence spontaneously accumulate in the cell nucleus, via its binding to DNA. By contrast, **Nanogel^{DOX}** needs to enter the cell by endocytosis, ending up in intracellular endosomal vesicles, hence the punctuated pattern. From these endosomes doxorubicin is gradually released by pH-accelerated cleavage of the hydrazone bonds, allowing to diffuse through the endosomal membrane and accumulate in the cell nucleus.

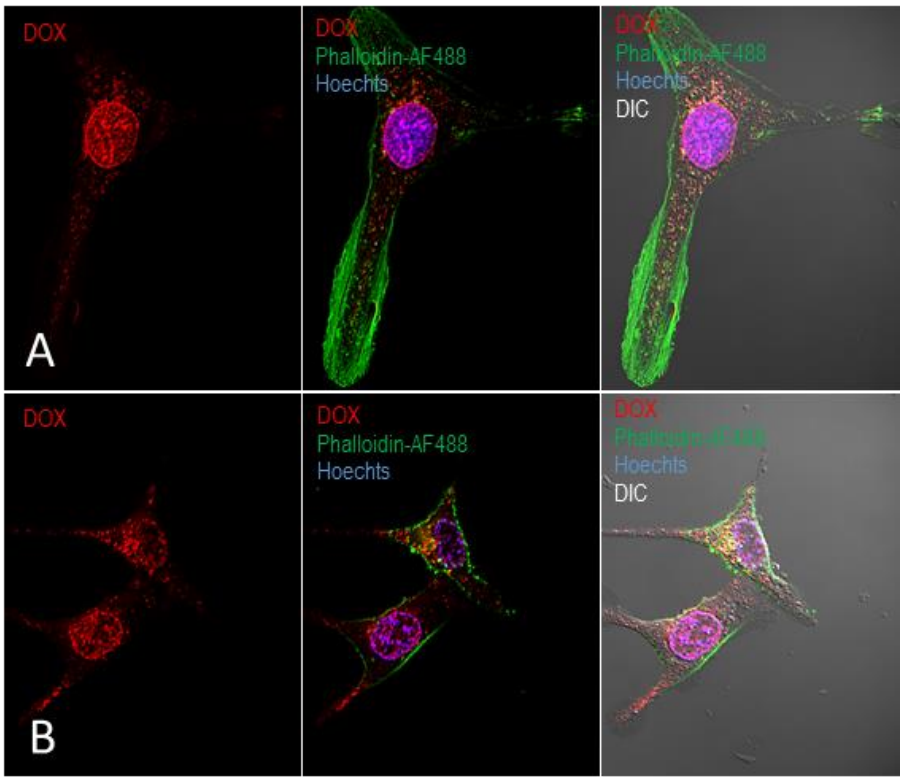

Figure 3. Confocal images of SKOV-3 cells incubated with soluble doxorubicin (A) and **Nanogel^{DOX}** (B) for 48 hours. Cell nuclei and membranes are depicted in blue and green respectively. Doxorubicin is visualized in red.

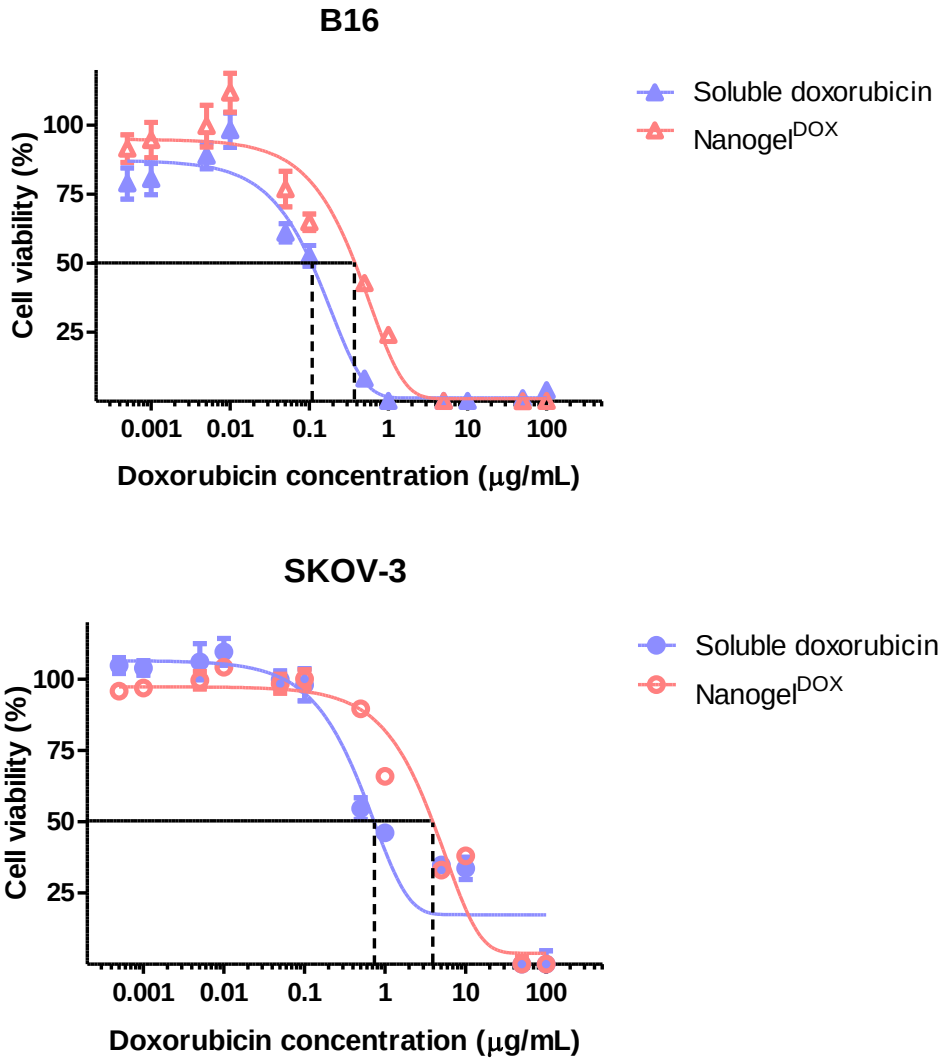

Figure 4. *In vitro* cytotoxicity evaluation on B16 (triangle) and SKOV-3 (circle) cells after 72 hours of incubation with different doses of soluble doxorubicin (blue) and **Nanogel^{DOX}** (red).

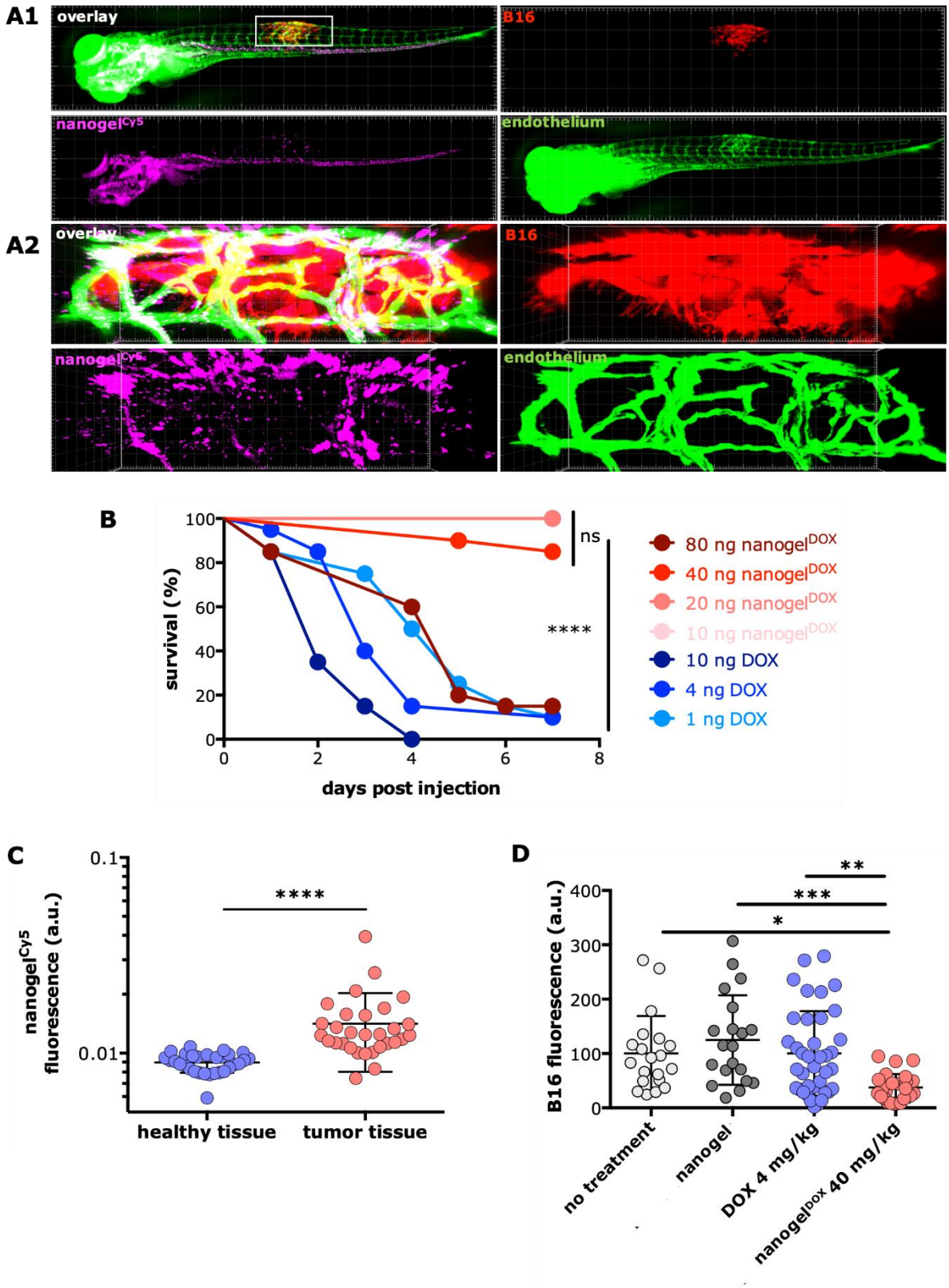

Figure 5. *In vivo* evaluation in zebrafish embryo. (A,C) **Nanogel^{Cy5}** accumulation into tumors (A) Fluorescence microscopy (A1) of a representative B16 tumor-bearing zebrafish embryo and (A2) corresponding confocal microscopy image (3D images calculated from a z-stack) of the tumor region. B16 melanoma cells are shown in red, zebrafish vascular endothelium in green and **Nanogel^{Cy5}** in violet. (B) Toxicity evaluation: Survival analysis of zebrafish embryo injected with different concentrations of doxorubicin either in free form

or **Nanogel^{DOX}**. n=20, Student´s t-test ****: p<0,0001 (C): Quantification of the fluorescent signal of **Nanogel^{Cy5}** in the area of the tumor or in an equivalent region of the neural tube without cancer cells. Student´s t test , n=30, ****: p<0,0001 (D) Therapeutic evaluation: Quantification of the fluorescent signal of cancer cells in xenotransplanted zebrafish embryo after treatment with doxorubicin as a free drug or **Nanogel^{DOX}**. Doxorubicin-free nanogels or diluting medium alone were used as controls. n(no treatment)= 20, n(blank nanogels)= 20, n(DOX)>38, n(nanogel^{DOX})>20. One way Anova, *: p<0,02, **: p<0,005, ***: p<0,0005.

Next, we investigated the cytotoxic activity of nanogel-conjugated doxorubicin by MTT assay in SKOV-3 and B16 mouse melanoma cells. In both cases, nanogel-conjugation resulted in a decrease in cytotoxic activity (**Figure 4**). This is a known phenomenon, whereas doxorubicin in free form is rapidly bioavailable, when conjugated to nanogels it has first to be released at low pH, a process that can explain the reduction in toxicity[55,56].

As a final part of this work we aimed to perform an *in vivo* screening of the therapeutic potential of **Nanogel^{DOX}**. For this purpose we made use of a zebrafish embryo ´pre-murine´ *in vivo* model. Zebrafish embryos are fully transparent which allows for whole animal imaging using standard fluorescence and microscopy equipment. This allows for straightforward investigation of the pharmacokinetics of fluorescently labelled structures at sub-cellular resolution, especially in combination with transgenic zebrafish with fluorescent tissues, such as eGFP-expressing vasculature, as used in our present study.
We first assessed whether the reduction in toxicity observed in cultured cells could also be detected in zebrafish embryo. For this, we intravenously (i.e. in the caudal vein) injected two days old embryos with different concentrations of doxorubicin either in free form or conjugated to nanogels and monitored the embryos survival in the following days. Doxorubicin alone was found to be toxic even at 1 mg/kg (1 ng doxorubicin) while **Nanogel^{DOX}** dramatically reduced its negative effects as a 40 mg/kg (40 ng doxorubicin) dose injected animals was found to be undistinguishable from mock injected controls (**Figure 5B**).
We next used a zebrafish xenograft tumor model to investigate tumor accumulation and tumor growth reduction in response to **Nanogel^{DOX}** treatment. In these experiments, we implanted B16 mouse melanoma cells, expressing RFP (red fluorescent protein) into the neural tube of zebrafish embryo. As the adaptive immune system is inactive during the first month of development, cells form other species can be xenografted and allowed to proliferate without facing rejection from the host. We focused on the localization of fluorescent nanogels after bloodstream injection in respect to zebrafish larvae xenotransplanted in the region of the neural tube with B16 cancer cells. Interestingly, the tumor region shows extensive neovascularization, evidenced by an irregular structure compared to the rectangular vasculature of healthy zebrafish tissue, interpenetrating the

red fluorescent tumor mass. This feature highlights the potential of this zebrafish xenograft model for studying the behavior of drug delivery systems in a physiological context and for investigating EPR-like tumor accumulation. Fluorescence imaging performed one day after nanoparticle injection revealed a significant increase in **Nanogel^{Cy5}** accumulation in the tumor area when compared to an equivalent region of the neural tube (**Figure 5A,C**).
Finally we tested the ability of **Nanogel^{DOX}** to inhibit the growth of xenografted B16 cells in zebrafish embryo. For this we first injected the cancer cells in the neural tube at two days post fertilization. The day after we injected into the caudal vein either 40 mg/kg (40 ng) of **Nanogel^{DOX}** or the highest dose of free drug that had moderate toxicity, 4 mg/kg (4 ng). As controls we included zebrafish larvae injected with doxorubicin-free nanogels or with the diluting medium. While free doxorubicin did not exhibit any effect, **Nanogel^{DOX}** were able to reduce the B16 fluorescence signal by half and therefore significantly reduce tumor growth (**Figure 5D**).

Conclusion

We demonstrated a straightforward route, based on activated esters, for the synthesis of core-crosslinked nanogels that contain hydrazide moieties in their core that can be used for doxorubicin conjugation. The resulting **Nanogel^{DOX}** provided accelerated drug release under acidic conditions. **Nanogel^{DOX}** could be endocytosed by cancer cells *in vitro* and thereby killing them, although with decreased activity relative to doxorubicin in soluble form. *In vivo* screening experiments in tumor-bearing zebrafish embryo indicated a dramatic reduction in systemic toxicity, but enhanced tumor accumulation and tumor growth reduction. Our findings also highlight the power of the zebrafish embryo tumor model for rapid screening of drug nanocarriers in a physiological context. In our future endeavors, we will further elaborate on PFP activated esters as scaffolds for drug conjugation and focus on the development of systems that contain a degradable crosslinker and include of cancer cell receptor targeting ligands at the hydrophilic polymer chain ends.

Acknowledgements

A.V.D., SB PhD fellow at FWO, thanks the Research Foundation-Flanders for a Ph.D. scholarship (grant number 1S01017N). BGDG acknowledges the FWO Flanders (grant number G044017N) for funding.

Supporting Information

Spectroscopic, chromatographic and supramolecular characterization.

Financial and competing interest disclosure

The authors declare no financial and/or competing interests.

References

1. Lee CC, Gillies ER, Fox ME, et al. A single dose of doxorubicin-functionalized bow-tie dendrimer cures mice bearing C-26 colon carcinomas. *Proc Natl Acad Sci*. 2006;103(45):16649-16654.

2. Minotti G. Anthracyclines: Molecular Advances and Pharmacologic Developments in Antitumor Activity and Cardiotoxicity. *Pharmacol Rev*. 2004;56(2):185-229.

3. Adimoolam MG, Amreddy N, Nalam MR, Sunkara M V. A simple approach to design chitosan functionalized Fe 3 O 4 nanoparticles for pH responsive delivery of doxorubicin for cancer therapy. *J Magn Magn Mater*. 2018;448:199-207.

4. Zhu Q, Jia L, Gao Z, et al. A tumor environment responsive doxorubicin-loaded nanoparticle for targeted cancer therapy. *Mol Pharm*. 2014;11(10):3269-3278.

5. Shafei A, El-Bakly W, Sobhy A, et al. A review on the efficacy and toxicity of different doxorubicin nanoparticles for targeted therapy in metastatic breast cancer. *Biomed Pharmacother*. 2017;95(June):1209-1218.

6. Brigger I, Dubernet C, Couvreur P. Nanoparticles in cancer therapy and diagnosis. *Adv Drug Deliv Rev*. 2002;54(5):631-651.

7. Griffin AM, Butow PN, Coates AS, et al. On the receiving end V: Patient perceptions of the side effects of cancer chemotherapy in 1993. *Ann Oncol*. 1996;7(2):189-195.

8. Mitra S, Gaur U, Ghosh P., Maitra A. Tumour targeted delivery of encapsulated dextran–doxorubicin conjugate using chitosan nanoparticles as carrier. *J Control Release*. 2001;74(1-3):317-323.

9. Allen TM. Drug Delivery Systems: Entering the Mainstream. *Science (80-)*. 2004;303(5665):1818-1822.

10. Danhier F. To exploit the tumor microenvironment: Since the EPR effect fails in the clinic, what is the future of nanomedicine? *J Control Release*. 2016;244:108-121.

11. Louage B, Zhang Q, Vanparijs N, et al. Degradable Ketal-based block copolymer nanoparticles for anticancer drug delivery: A systematic evaluation. *Biomacromolecules*. 2015;16(1):336-350.

12. Kasmi S, Louage B, Nuhn L, et al. Transiently Responsive Block Copolymer Micelles Based on N -(2-Hydroxypropyl)methacrylamide Engineered with Hydrolyzable

Ethylcarbonate Side Chains. *Biomacromolecules*. 2016;17(1):119-127.

13. Nel A, Ruoslahti E, Meng H. New Insights into "permeability" as in the Enhanced Permeability and Retention Effect of Cancer Nanotherapeutics. *ACS Nano*. 2017;11(10):9567-9569.

14. Rafiyath SM, Rasul M, Lee B, Wei G, Lamba G, Liu D. Comparison of safety and toxicity of liposomal doxorubicin vs. conventional anthracyclines: a meta-analysis. *Exp Hematol Oncol*. 2012;1(1):10.

15. Peer D, Karp JM, Hong S, Farokhzad OC, Margalit R, Langer R. Nanocarriers as an emerging platform for cancer therapy. *Nat Nanotechnol*. 2007;2(12):751-760.

16. Cao XT, Le CMQ, Thi HHP, Kim GD, Gal YS, Lim KT. Redox-responsive core cross-linked prodrug micelles prepared by click chemistry for ph-triggered doxorubicin delivery. *Express Polym Lett*. 2017;11(10):832-845.

17. Kamaly N, Yameen B, Wu J, Farokhzad OC. Degradable controlled-release polymers and polymeric nanoparticles: Mechanisms of controlling drug release. *Chem Rev*. 2016;116(4):2602-2663.

18. Lostalé-Seijo I, Louzao I, Juanes M, Montenegro J. Peptide/Cas9 nanostructures for ribonucleoprotein cell membrane transport and gene edition. *Chem Sci*. 2017;8(12):7923-7931.

19. Priegue JM, Lostalé-Seijo I, Crisan D, Granja JR, Fernández-Trillo F, Montenegro J. Different-Length Hydrazone Activated Polymers for Plasmid DNA Condensation and Cellular Transfection. *Biomacromolecules*. 2018;19(7):2638-2649.

20. Kamaly N, Xiao Z, Valencia PM, Radovic-Moreno AF, Farokhzad OC. Targeted polymeric therapeutic nanoparticles: design, development and clinical translation. *Chem Soc Rev*. 2012;41(7):2971-3010.

21. Mitragotri S, Burke PA, Langer R. Overcoming the challenges in administering biopharmaceuticals: formulation and delivery strategies. *Nat Rev Drug Discov*. 2014;13(9):655-672.

22. Shi J, Kantoff PW, Wooster R, Farokhzad OC. Cancer nanomedicine: progress, challenges and opportunities. *Nat Rev Cancer*. 2017;17(1):20-37.

23. Shi J, Schellinger JG, Pun SH. Engineering biodegradable and multifunctional peptide-based polymers for gene delivery. *J Biol Eng*. 2013;7(1):1-10.

24. Blencowe CA, Russell AT, Greco F, Hayes W, Thornthwaite DW. Self-immolative linkers in polymeric delivery systems. *Polym Chem*. 2011;2(4):773-790.

25. Riber CF, Smith AAA, Zelikin AN. Self-Immolative Linkers Literally Bridge Disulfide Chemistry and the Realm of Thiol-Free Drugs. *Adv Healthc Mater*. 2015;4(12):1887-1890.

26. Bartolami E, Bouillon C, Dumy P, Ulrich S. Bioactive clusters promoting cell penetration and nucleic acid complexation for drug and gene delivery applications: From designed to self-assembled and responsive systems. *Chem Commun*. 2016;52(23):4257-4273.

27. Peterson JJ, Meares CF. Cathepsin substrates as cleavable peptide linkers in bioconjugates, selected from a fluorescence quench combinatorial library. *Bioconjug Chem*. 1998;9(5):618-626.

28. Sevenich L, Joyce JA. Pericellular proteolysis in cancer. *Genes Dev*. 2014;28(21):2331-2347.

29. Kalia J, Raines RT. Hydrolytic stability of hydrazones and oximes. *Angew Chemie - Int Ed*. 2008;47(39):7523-7526.

30. Kölmel DK, Kool ET. Oximes and Hydrazones in Bioconjugation: Mechanism and Catalysis. *Chem Rev*. 2017;117(15):10358-10376.

31. Crielaard BJ, Rijcken CJF, Quan L, et al. Glucocorticoid-loaded core-cross-linked polymeric micelles with tailorable release kinetics for targeted therapy of rheumatoid arthritis. *Angew Chemie - Int Ed*. 2012;51(29):7254-7258.

32. Gyarmati B, Némethy Á, Szilágyi A. Reversible disulphide formation in polymer networks: A versatile functional group from synthesis to applications. *Eur Polym J*. 2013;49(6):1268-1286.

33. Phillips DJ, Gibson MI. Redox-Sensitive Materials for Drug Delivery: Targeting the Correct Intracellular Environment, Tuning Release Rates, and Appropriate Predictive Systems. *Antioxid Redox Signal*. 2014;21(5):786-803.

34. Meng X, Gao M, Deng J, et al. Self-immolative micellar drug delivery: The linker matters. *Nano Res*. 2018;1:1-13.

35. Jia X, Zhao X, Tian K, et al. Fluorescent Copolymer-Based Prodrug for pH-Triggered Intracellular Release of DOX. *Biomacromolecules*. 2015;16(11):3624-3631.

36. Godula K, Bertozzi CR. Synthesis of glycopolymers for microarray applications via ligation of reducing sugars to a poly(acryloyl hydrazide) scaffold. *J Am Chem Soc*. 2010;132(29):9963-9965.

37. McKinnon DD, Domaille DW, Cha JN, Anseth KS. Bis-aliphatic hydrazone-linked hydrogels form most rapidly at physiological pH: Identifying the origin of hydrogel properties with small molecule kinetic studies. *Chem Mater*. 2014;26(7):2382-2387.

38. Vasey PA, Duncan R, Kaye SB, Cassidy J. 929 Clinical phase I trial of PK1 (HPMA co-polymer doxorubicin). *Eur J Cancer*. 1995;31(November):S193.

39. Mitchell MJ, Jain RK, Langer R. Engineering and physical sciences in oncology: challenges and opportunities. *Nat Rev Cancer*. 2017;17:659-675.

40. Das A, Theato P. Activated Ester Containing Polymers: Opportunities and Challenges for the Design of Functional Macromolecules. *Chem Rev*. 2016;116(3):1434-1495.

41. Vanparijs N, Nuhn L, Paluck SJ, et al. Core/shell protein-reactive nanogels via a combination of RAFT polymerization and vinyl sulfone postmodification. *Nanomedicine*. 2016;11(20):2631-2645.

42. De Coen R, Vanparijs N, Risseeuw MDP, et al. pH-Degradable Mannosylated Nanogels for Dendritic Cell Targeting. *Biomacromolecules*. 2016;17(7):2479-2488.

43. Nuhn L, Vanparijs N, De Beuckelaer A, et al. pH-degradable imidazoquinoline-ligated nanogels for lymph node-focused immune activation. *Proc Natl Acad Sci*. 2016;113(29):8098-8103.

44. Nuhn L, Hirsch M, Krieg B, et al. Cationic nanohydrogel particles as potential siRNA carriers for cellular delivery. *ACS Nano*. 2012;6(3):2198-2214.

45. Evensen L, Johansen PL, Koster G, et al. Zebrafish as a model system for characterization of nanoparticles against cancer. *Nanoscale*. 2016;8(2):862-877.

46. Zhang L, Lu J, Qiu L. Synergistic effects of A-B-C-type amphiphilic copolymer on reversal of drug resistance in MCF-7/ADRbreast carcinoma. *Int J Nanomedicine*. 2016;11:5205-5220.

47. Maxwell IA, Morrison BR, Napper DH, Gilbert RG. Entry of free radicals into latex particles in emulsion polymerization. *Macromolecules*. 1991;24(7):1629-1640.

48. Etrych T, Jelínková M, Íhová B, Ulbrich K. New HPMA copolymers containing doxorubicin bound via pH-sensitive linkage: Synthesis and preliminary in vitro and in vivo biological properties. *J Control Release*. 2001;73(1):89-102. doi:10.1016/S0168-3659(01)00281-4

49. Talelli M, Barz M, Rijcken CJF, Kiessling F, Hennink WE, Lammers T. Core-

crosslinked polymeric micelles: Principles, preparation, biomedical applications and clinical translation. *Nano Today*. 2015;10(1):93-117. doi:10.1016/j.nantod.2015.01.005

50. Nuhn L, Van Hoecke L, Deswarte K, et al. Potent anti-viral vaccine adjuvant based on pH-degradable nanogels with covalently linked small molecule imidazoquinoline TLR7/8 agonist. *Biomaterials*. 2018;178:643-651.

51. Nuhn L, Van Herck S, Best A, et al. FRET Monitoring of Intracellular Ketal Hydrolysis in Synthetic Nanoparticles. *Angew Chemie Int Ed*. 2018;57(33):10760-10764.

52. Motlagh NSH, Parvin P, Ghasemi F, Atyabi F. Fluorescence properties of several chemotherapy drugs: doxorubicin, paclitaxel and bleomycin. *Biomed Opt Express*. 2016;7(6):2400-2406.

53. Riddles PW, Blakeley RL, Zerner B. Ellman's reagent: 5,5'-dithiobis(2-nitrobenzoic acid)—a reexamination. *Anal Biochem*. 1979;94(1):75-81.

54. Shi Y, Lammers T, Storm G, Hennink WE. Physico-chemical strategies to enhance stability and drug retention of polymeric micelles for tumor-targeted drug delivery. *Macromol Biosci*. 2017;17(1):1600160.

55. J. RJ, W. MJ, Hirotaka E, et al. Versatile Loading of Diverse Cargo into Functional Polymer Capsules. *Adv Sci*. 2015;2(1-2):1400007.

56. Talelli M, Iman M, Varkouhi AK, et al. Core-crosslinked polymeric micelles with controlled release of covalently entrapped doxorubicin. *Biomaterials*. 2010;31(30):7797-7804.